UNCLASSIFIED

Defense Technical Information Center
Compilation Part Notice

ADP012201

TITLE: Sol-Gel Synthesis and Characterization of Neodymium-Ion Doped Nanostructured Titania Thin Films

DISTRIBUTION: Approved for public release, distribution unlimited

This paper is part of the following report:

TITLE: Nanophase and Nanocomposite Materials IV held in Boston, Massachusetts on November 26-29, 2001

To order the complete compilation report, use: ADA401575

The component part is provided here to allow users access to individually authored sections of proceedings, annals, symposia, etc. However, the component should be considered within the context of the overall compilation report and not as a stand-alone technical report.

The following component part numbers comprise the compilation report:
ADP012174 thru ADP012259

UNCLASSIFIED

Mat. Res. Soc. Symp. Proc. Vol. 703 © 2002 Materials Research Society V5.2

SOL-GEL SYNTHESIS AND CHARACTERIZATION OF NEODYMIUM-ION DOPED NANOSTRUCTURED TITANIA THIN FILMS

Andrew Burns[(1)], W. Li[(1)], C. Baker[(1)] and S.I. Shah[(1,2)]
[(1)]Department of Material Science and Engineering
[(2)]Department of Physics and Astronomy
University of Delaware, Newark, DE 19716

ABSTRACT

Nd doped TiO_2 nanostructured thin films were prepared by sol-gel technique on quartz and Si substrates using $TiCl_4$ precursor. As-deposited amorphous films were annealed to form anatase phase in the thin films. The film grain size increased with annealing temperature. Above 800°C, rutile began to segregate and the grain size decreased slightly.

The photodegradation of 2-chlorophenol (2-CP) was studied. Doping TiO_2 with Nd^{+3} reduced the photodegradation time. The difference in the ionic radii of Nd^{+3} and Ti^{+4} and the oxygen affinities of Nd and Ti were responsible for this effect. These differences help promote electron trapping, thereby increasing the lifetime of the holes which are responsible for the oxidation of 2-CP.

1. INTRODUCTION

Contaminants from industrial waste pose a major environmental threat to air and water. As of 1990, the EPA estimated that 10,000 U.S. public water sources contained pesticides or other contaminants linked to cancer and to kidney and nervous system damage. A method is needed to effectively neutralize these and other pollutants. Semiconductor photocatalysis offers a promising solution. Nanostructured semiconductors effectively catalyze aqueous reactions, which break down harmful organic pollutants to relatively harmless constituent chemicals.

Semiconductor photocatalysis takes advantage of the valence/conduction bandgap specific to semiconductor molecules. Incoming photons with energies at or above the bandgap will cause valence electrons to become excited and move to the conduction shell, leaving holes in the valence band. These excited charge carriers can react with molecules adsorbed on the semiconductor surface, thus acting as catalysts [1]. There are several competing effects, which limit the effectiveness of the catalysts. Most of the activated charge carriers will undergo recombination before reaching the surface to interact with adsorbed molecules. Up to 90% of the generated carriers are lost within a nanosecond of generation. As the grain size decreases, the probability of volumetric recombination also decreases, along with creating greater surface area for adsorption, thus making nanostructured systems particularly viable. However, there is an optimum in the particle size. As the particle size decreases, the probability of surface recombination increases, thereby limiting the minimum particle size.

Among the most viable nanoparticles for photocatalysis applications is titanium dioxide. TiO_2 is stable in aqueous media and is tolerant of both acidic and alkaline solutions. It is inexpensive, recyclable, reusable and relatively simple to produce. It also forms nanostructures more readily than other catalysts. Furthermore, its bandgap

includes the redox potential for the $H_2O/•OH$ reaction (-2.8V), thus allowing degradation of many organic compounds [2]. Unfortunately, the large (3.2 eV) bandgap of TiO_2, lies in the UV range, so that only 5-8% of sunlight photons have the requisite energy to activate the catalyst. A visible light (λ = 400-800nm) catalyst would be much more effective and efficient.

There are several ways to increase the efficiency of TiO_2 as a catalyst. Decorating the particle surface with noble metals increases the surface charge transfer by stabilizing the electron-hole pairs once they reach the catalyst surface. Another option is sensitization in which catalyst is coated with a lower-bandgap material (organic dyes, CdS, etc.) which, upon activation, creates electron-hole pairs which can be transferred to the host TiO_2 and made available for photocatalysis. A related field of interest is photovoltaics, which uses the principle of dye sensitized TiO_2 [3]. Unfortunately, all of the known sensitizers are toxic or unstable in aqueous medium, thus making them inappropriate for application in photocatalysis. Doping the catalyst with certain metal ions can increase its effectiveness by introducing trapping sites. Trapping of electrons or holes at these sites effectively increases their lifetime and, therefore, the probability that they will reach the surface without suffering recombination and participate in the desired photocatalysis reaction. Some possible dopant ions include Nd^{+3}, Cr^{+3}, Pd^{+4} and Fe^{+3}. Selection of the dopants depends on the reaction of interest. Not all dopants work efficiently for all reactions. For example, Fe^{+3} works well for the catalysis of $CHCl_3$ [4] but not for 2-chlorophenol [5].

This study describes the preparative methodology used in making TiO_2 nanostructured thin films on quartz substrates via sol-gel method. The purpose of this study was to determine the effects of preparation conditions and Neodymium dopant concentration on nanostructured thin film titania. Effects on the physical and photochemical properties are investigated.

2. EXPERIMENTAL PROCEDURES

The Neodymium-doped TiO_2 nanostructured thin films were synthesized from titanium tetrachloride (Fluka 98%) and Neodymium (III) acetylacetonate hydrate (Aldrich) precursors in ethanol (Pharmco 200 Proof) by the sol-gel method previously described [6]. The Nd-precursor was massed to yield the desired molar ratios with TiO_2 and sonicated in 20ml ethanol to yield a homogenous opaque purple solution. 2 ml of $TiCl_4$ was added drop-wise to this solution. The reaction was carried out at room temperature under a fume hood due to the large amount of HCl gas evolved in this reaction. The product was allowed to rest until all HCl gas had dissipated, leaving a transparent, slightly viscous, yellow solution. This solution was allowed to evaporate for several hours to remove excess ethanol.

For physical and compositional measurements, quartz substrates and Boron (P-Type) doped silicon wafers (VSI) were dip coated in the solution and removed at approximately 2cm/min. For photodegradation experiments, 1" x 10" quartz tubes were coated by a similar method. These films were allowed to air dry in a desiccator (to avoid hydrolysis) overnight, followed by calcination in a stainless steel tubular furnace operating between 500° and 875°C under flowing O_2. Crystal growth was analyzed via X-ray diffraction and SEM.

Structural characterization of the doped and undoped TiO_2 samples was carried out by X-ray diffraction (XRD). θ-2θ scans were recorded using Cu K_α radiation in a Rigaku D-Max B diffractometer equipped with a graphite crystal monochromator. Precise 2θ positions and the full width at half maxima of the diffraction peaks were obtained by using XFIT software [7]. Compositions of the samples were determined by X-ray photoelectron spectroscopy (XPS) and energy dispersive X-ray spectroscopy (EDS). A SSI-M Probe XPS was used employing Al K_α exciting radiation. In addition to the survey scans, high resolution scans in the Ti 2p, Nd 4d, O 1s, and C 1s regions were also recorded. The Ti 2p and dopant 4d regions were used to measure the composition of the nanoparticles and to ascertain the valence states of Ti and the dopant. The doping concentration in TiO_2 was also confirmed by a JEOL energy dispersive x-ray spectrometer using a 20.0keV electron beam for X-ray excitation. The measurement of average particle size and surface morphology were performed by means of Scanning Electron Microscopy (SEM) in a JEOL SEM operating at 15.0 kV.

Photodegradation experiments were performed in the photocatalytic reactor system. This bench-scale system consisted of a cylindrical Pyrex-glass cell, 12 cm inside diameter and 30 cm high, with an inside reflective surface. A 100 Watts Hg lamp was used which was immersed in the solution with the cold air-cooling jacket. The maximum energy emission of UV at the wavelength of 365 nm was achieved in 4 minutes after the lamp was turned on. At the cooling jacket, an energy density of 5.3 mW/cm^2 was measured and the photon flux was calculated to be 4.42×10^{-4} Einstein/min. An aqueous solution (1000 mL) of 2-CP and the quartz tube coated with 10 mg TiO_2 nanoparticles were placed in the photoreactor cell. A magnetic stirrer was used in the suspension and O_2 was supplied through compressed air for the oxidation reaction. During illumination, the pH value of whole suspension was controlled at 9.5. After illumination, samples were collected at regular intervals in a test-tube and each sample suspension was filtered by 0.2-μm filter and then analyzed by high performance liquid chromatograph (HPLC).

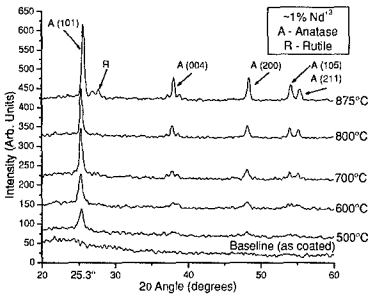

Fig.1. XRD patterns of as-deposited and annealed Nd-doped TiO_2 nanostructured thin films.

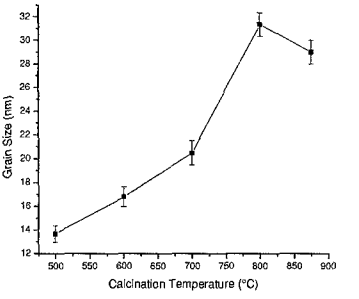

Fig.2. Grain size of Nd-doped TiO_2 films as a function of the calcination temperature.

The total organic carbon (TOC) of a sample solution was measured at constant irradiation time intervals using a DC-190 high temperature TOC analyzer. The Cl^- ion was analyzed by ion chromatograph (Dionex Bio LC Chromatography) equipped with an electrochemical detector and a Dionex PAX-100 metal-free anion column (25 cm long, 4.6 mm I.D.). The eluent solution was a mixture of 80 % H_2O, 10% acetonitrile and 10% 191-mM NaOH. The flow rate was 1 mL/min and the injection loop volume was 50 μL. The activity of the photocatalytic decomposition of 2-CP was again estimated from the yield of carbon dioxide, determined gravimetrically as $BaCO_3$, from the yield of carbon dioxide as decreasing results of electric conductivity for $Ba(OH)_2$ solution. HCO_3^- in a sample solution was measured by ion and liquid chromatography.

3. RESULTS

Figure 1 shows the X-ray diffraction pattern obtained from films grown on quartz substrates and annealed at temperatures ranging from 500 °C to 875 °C. The as-grown thin film was amorphous and did not show and x-ray structure. From 500°C to 700°C only peaks related to anatase structure were evident. Above 800°C, films contained a mixture of both the anatase and rutile phases of TiO2. The anatase (101) peak was used to determine the grain size by Scherrer's formula [8]. The results of the grain size analysis are presented in Fig. 2. The grain sizes increases at first, as the calcination temperature is raised from 500°C to 800°C and then decreases slightly as the calcination temperature is further raised above 800°C. The grain size ranges between 14 to 30 nm. The initial increase in grain size with temperature is as expected. Slight decrease in the grain size above 800°C correlates with the formation of rutile phase. Such grain size decrease has been reported previously and explained in terms of the intragranular rutile segregation in the anatase matrix [9].

No Nd related phases were observed by the x-ray diffraction analysis. This suggests that there is no Nd segregation in amounts large enough to be detected by XRD. Most of the Nd resides as substitutional or interstitial impurity.

The surface structure of the films was analyzed by SEM, as shown in Fig. 3. The particle sizes found by SEM generally concur with those determined by XRD, though some agglomeration is apparent. The surfaces of the samples are flat with no noticeable protrusions commonly associated with dip coating methods.

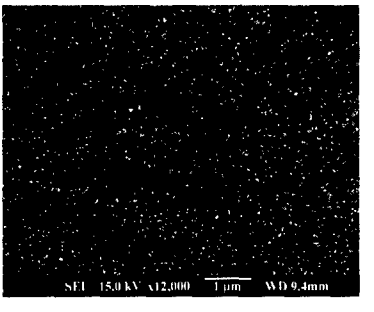

Fig. 3. SEM micrograph of the Nd-doped TiO_2 film surface.

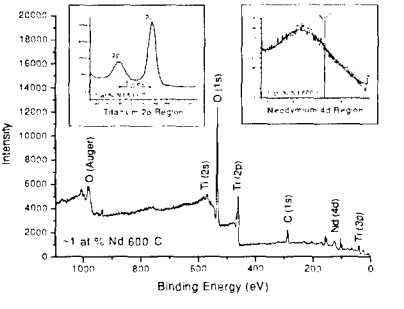

Fig. 4. XPS survey and high resolution Ti 2p and Nd 4d regions.

The valence state and the cation composition in the films were determined by X-ray photoelectron spectroscopy and energy dispersive spectroscopy. Fig. 4 shows the XPS survey for a Nd doped sample. Only peaks associated with Ti, O and Nd were observed. Nd concentration was measured to be about 1 at%. The inserts in Fig. 5 are the magnified Ti 2p and Nd 4d regions. The Ti 2p region shows two peaks located at 458.5 eV and 464.2 eV, respectively. The peaks for metallic Ti^0 are expected at 455 ($2p_{3/2}$) and 459 ($2p_{1/2}$) eV [10]. The shifts in Ti ($2p_{3/2}$) and Ti ($2p_{1/2}$) peak positions are due to the presence of tetravalent Ti^{4+}, as expected in TiO_2. The change in the separation between the Ti ($2p_{3/2}$) and Ti ($2p_{1/2}$) peaks is also consistent with the formation of TiO_2 [10,11].

The analysis of the Nd 4d region is relatively problematic due to the low concentration; however, the peak is shifted from the metallic position indicating Nd-O bonding. The detailed analysis of this peak is currently being carried out. The composition of the cations was confirmed by EDX analysis.

The photodegradation experiments were carried out on samples doped with about 1% Nd. The activities for the photodegradation for 2-CP are presented in Fig. 5. The figure also shows the photoactivity of the undoped Degussa P25 standard. The results show that the activities for the photodegradation of 2-CP have been enhanced with the addition of Nd. The time of 90% destruction of 2-CP has been reduced to 25 minutes from 60 minutes in the case of Degussa P25. Assuming that the fraction of absorbed photons by TiO_2 is 1, the apparent quantum yields can be calculated. The apparent quantum yields are shown in Table I. The quantum yield of 2-CP suspension with Nd doped TiO_2 catalyst is almost 2.5 times that of Degussa P25.

For the oxidation of 2-chlorophenol, the trapping of electrons is critical. In nanostructured TiO_2 thin films, electron trapping reduces surface recombination and allows holes to diffuse to the particle surface and participate in the oxidation reaction. Any dopant that effectively increases the localized positive charge will improve the oxidation of chlorophenol. The effective ionic radii of Nd^{3+} and Ti^{4+}, are 0.983 Å and 0.605 Å, respectively [12,13]. The large difference in the ionic radii causes dilation of the lattice and localized charging. The high oxygen affinities of Nd cause a strong

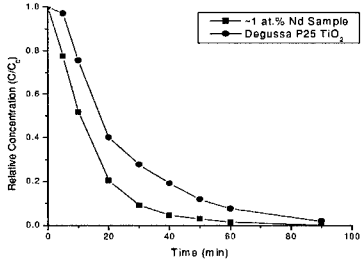

Fig. 5. 2-CP photodegradation with Nd-doped TiO_2 and Degussa P25 standard TiO_2.

Table I: Photodegradation Analysis

Catalyst	Initial Rate $10^6 \cdot R_{in}$ (mol/min)	Photon Flux $10^4 R_{o_{(365)}}$ (Einstein/min)	Quantum Yield $-10^2 \Phi_{2CP} = R_{in}/R_{o_{(365)}}$
~1 at.% Nd Dopant	15.5	4.42	3.5
Degussa P25	11.7	4.42	2.7

dopant-oxygen bond. This effectively creates a localized positive charge around Ti and/or forms an oxygen vacancy. Both of these possibilities help form electron traps and increase the lifetime of holes.

4. CONCLUSION

We have prepared Nd doped TiO_2 nanostructured thin films on quartz and Si substrates by standard sol-gel technique using $TiCl_4$ as precursor. As-deposited films were amorphous and required a post-deposition calcination. Calcination caused anatase formation. The anatase grain size grew with calcination temperature. Above 800°C, rutile started to segregate from the anatase phase and the anatase grain size decreased slightly.

Photocatalysis measurement on the degradation of 2-CP indicated a reduction in the degradation time by the addition of Nd to TiO_2. This reduction is related to the difference in the ionic radii of Nd^{+3} and Ti^{+4} and the oxygen affinities of Nd and Ti. The larger Nd^{+3} ionic radius causes localized charge perturbations and the higher oxygen affinity of Nd induced the formation of oxygen vacancy. Both these effects help promote electron trapping, increasing the lifetime of the holes which are responsible for the oxidation of 2-CP.

5. REFRERENCES

1. D. Beydoun, R. Amal, G. Low, S. McEvoy, Journal of Nanoparticle Research 1: 439-458, Kluwer Academic Publishers, Netherlands
2. Aruna 1996. Journal of Materials Synthesis and Processing **4**(3), 175-179.
3. U. Bach, D. Lupo, P. Comte, J.E. Moser, F. Weissortel, J. Salbeck, H. Spreitzer, and M. Gratzel, Nature **395**, 583 (1998).
4. Z. Zhang, C. Wang, R. Zakaria, and J. Ying, J. Phys. Chem. B **102**, 10871 (1998).
5. W. Li, S. Ismat Shah, C.-P. Huang, O. Jung and C. Ni, to be published in J. Appl. Phys.
6. Y. Zhou, C.Y. Wang, H.J. Liu, Y.R. Zhu, Z.Y. Chen, Materials Science and Engineering B**67**, 95 (1999).
7. Freeware form http://www.ccp14.ac.uk/tutorial/xfit-95/
8. B.D. Cullity, Elements of X-Ray Diffraction (Addison-Wesley, Menlo Park, CA 1978).
9. L.H. Edelson and A.M. Glaeser, J. Amer, Ceram. Soc. **71**, 225(1988).
10. C.D. Wagner, W.M. Riggs, L.E. Davis, J.F. Moulder, and G.E. Muilenberg (Eds), Handbook of X-ray Photoelectron Spectroscopy (Perkin-Elmer corporation, 1979).
11. S.K. Sen, J. Riga, and J. Verbist, Chem. Phys. Lett. **39**, 560 (1976).
12. R.D. Shannon, Acta Crystallogr. Sect. A **32**, 751 (1976).
13. R.D. Shannon and C.T. Prewitt, Acta Crystallogr. Sect. B **25**, 925 (1969).